Effects of Laser Pulse Duration on Pulse Laser Micro Polishing

ICOMM
2012
No. 112

Madhu Vadali[1], Chao Ma[2], Neil A. Duffie[3], Xiaochun Li[4], and Frank E. Pfefferkorn[5].

[1]Madhu Vadali; Mechanical Engr., University of Wisconsin - Madison; e-mail: vadali@wisc.edu
[2]Chao Ma; Mechanical Engr., University of Wisconsin - Madison; e-mail: cma25@wisc.edu
[3]Neil A. Duffie; Mechanical Engr., University of Wisconsin - Madison; e-mail: duffie@engr.wisc.edu
[4]Xiaochun Li; Mechanical Engr., University of Wisconsin - Madison; e-mail: xcli@engr.wisc.edu
[5]Frank E. Pfefferkorn; Mechanical Engr., University of Wisconsin - Madison; e-mail: pfefferk@engr.wisc.edu.

ABSTRACT

Pulsed laser micro polishing (PLµP) has been shown to be an effective method of polishing micro metallic parts whose surface roughness can approach the feature size. This paper will describe the influence of laser pulse duration on surface roughness reduction during PLµP. It will be shown that longer pulse durations attenuate longer wavelength features, with corresponding deeper yet small melt depths and that those pulse durations may result in convective flows, introducing additional short wavelength features, yet significantly reducing the average surface roughness. For this purpose, near-infrared laser pulses have been used to polish Ti6Al4V surfaces produced using the micro end milling process.

INTRODUCTION

Pulsed laser micro polishing (PLµP) is a non-contact surface smoothening process suitable for metallic parts of micro/meso scales, where conventional polishing methods are unproductive and/or uneconomic. In PLµP, laser pulses irradiate the surface. Each pulse results in melting followed by damped oscillations of the melted surface due to the forces of surface tension and viscosity. If the oscillations damp out within the time that the surface is molten (melt duration, t_m), a smoother surface will result upon solidification [1, 2].

Continuous-wave (CW) laser polishing has been investigated on macro-scale metal parts [3, 4] with positive results. However, this can result in melt-depths and heat affected depths of 100s of microns [5]. This may not be suitable for devices with dimensions measured in 10s to 100s of microns. Pulsed laser polishing enables better control of melt depth and heat affected zone.

Past research on laser induced surface modification and surface finish indicate that reduction of surface roughness is possible at pulse durations less than 200 ns and spot sizes of few hundreds of microns[6, 7]. Other studies include laser induced surface finish of titanium for bio-implants[8, 9] and micro-roughness reduction of tungsten films in the IC industry[10]. More recently, Perry et al.[11-13] have demonstrated that pulsed laser micro-polishing (PLµP) with pulse durations of 300-650ns and a spot size of 60µm is a method by which the surface roughness of microfabricated and micro milled parts can be effectively reduced.

Analytical models are available that describe the dynamics of the melt pool [6-8]. These models are based on spatial Fourier analysis of the surfaces and examination of Navier-Stokes equation for each Fourier component. Perry et al. [11-13] have proposed a critical frequency, f_{cr}, which describes the cutoff point in the spatial frequency content of the surface, above which a significant reduction in the amplitude is expected. The critical frequency is a function of the duration of the molten state and is given by:

$$f_{cr} = \left(\frac{\rho}{8\pi^2 \mu t_m} \right)^{\frac{1}{2}} \quad (1)$$

Recently, the authors have extended the concept of critical frequency to develop an integrated fluid flow and heat transfer model to predict the surface finish achievable by PLµP on a given surface and laser pulse duration [14]. In this model, it is assumed that convection and radiation are negligible compared to conduction. The surface topography is transformed into spatial Fourier components. Once molten, these spatial frequency components can be assumed to oscillate like stationary capillary waves. The amplitude, $\zeta(f_x,f_y)$, of a spatial frequency component (f_x, f_y) decays exponentially with time [15]. The amplitude of interest in PLµP is the amplitude of a spatial frequency component at the end of melt duration, t_m and is given by:

$$\zeta (f_x,f_y)_{\text{polished}} = \zeta (f_x,f_y)_{\text{unpolished}} \, e^{-\left[(f_x/f_{cr})^2 + (f_y/f_{cr})^2 \right]} \quad (2)$$

Equations (1) and (2) show that the surface finish is significantly dependent on the surface melt duration which is governed by the laser pulse duration and the material properties. With longer laser pulses, the surface of a given material is molten for a longer time. This gives more time for the oscillations to damp out and a smoother finish can be expected.

Nusser et al. recently investigated the influence of two pulse durations (164ns and 1.25µs) on pulsed laser micro polishing of tool steel and observed that polishing at 1.25µs can smoothen lower spatial frequencies than polishing at 164ns [16]. In the current work, the authors aim at understanding the effects of laser pulse duration with the aid of PLµP experiments at three different pulse durations viz.,

· corresponding author

650ns, 1.91μs and 3.6μs. Experiments will be carried out on surfaces produced using micro end milling process on Ti6Al4V alloy. The cross sections of the polished region have been imaged to derive more knowledge about these effects and, in turn, about the process. Ti6Al4V has been chosen because of its wide applications in medical implants [17-20].

THEORETICAL PREDICTIONS

The surface finish prediction model [14], summarized in Fig. 1, is employed on each of the surfaces to theoretically estimate the effect of laser pulse duration on surface finish. The estimated melt durations and critical frequencies for the three pulse durations are listed in Table 1. The roughness of the surface was characterized using average surface roughness metric S_a, after filtering the waviness of the surface using a high pass Gaussian spatial filter with a waviness cut-off frequency, f_c, of 12.5mm^{-1} (cut-off wavelength λ_c = 0.08mm) [21, 22]. Table 2 shows the predicted polished roughness and percentage reductions in the average surface roughness for the three pulse durations. Fig. 2 shows the overlaid plots of the predicted spatial spectra after PLμP for the three pulse durations.
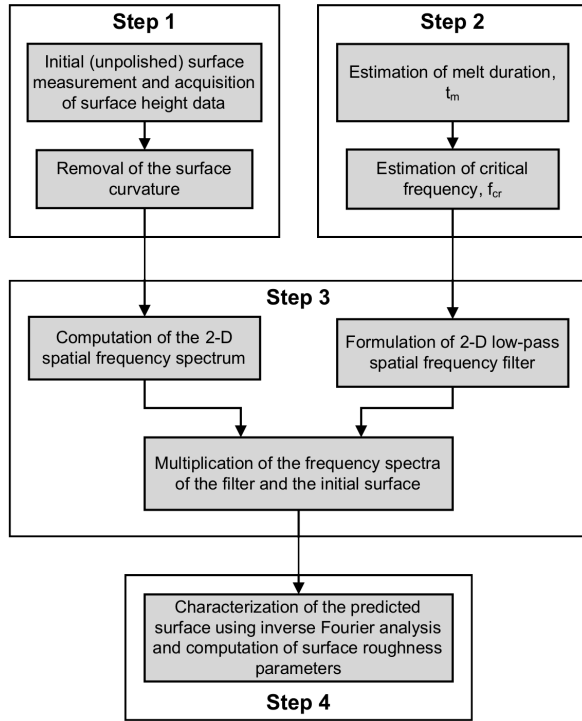

Fig. 1: PLμP surface finish prediction methodology

Table 1: Estimated melt durations and critical frequencies

Pulse duration (μs)	Maximum melt duration, $t_{m\text{-}max}$ (μs)	Critical frequency, f_{cr} (mm^{-1})
0.65	1.164	115
1.91	2.980	72
3.60	4.982	56

Table 2: Predicted (polished) roughness and reductions

Pulse duration (μs)	Sa-Unpolished (nm)	Sa-Predicted (nm)	Reduction in Sa (%)
0.65	193.9	138.0	18.6
1.91	211.6	127.5	39.7
3.6	206.5	94.4	54.3

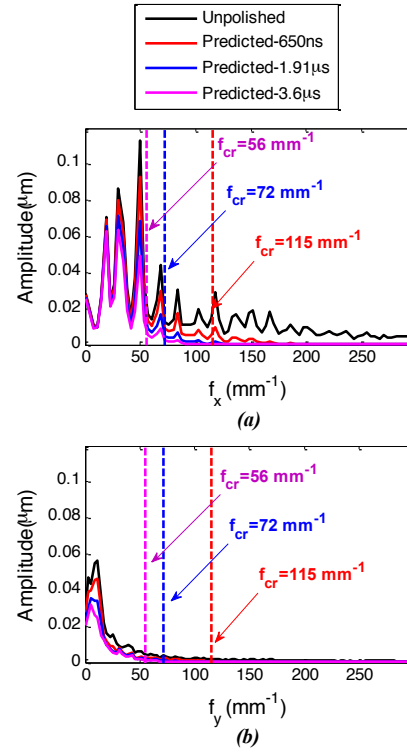**Fig. 2: Overlapped 2-D frequency spectra of unpolished, and polished (650ns, 1.91μs & 3.6μs). (a) Projected x-frequency spectra; (b) Projected y-frequency spectra**

EXPERIMENTAL SETUP AND PROCEDURES

A. EQUIPMENT

The basic experimental setup is illustrated in Fig. 3. Two lasers were used for experimentation: (1) A 1064nm, 250W (CW) Nd:YAG laser (Lee Lasers, Model: 8250MQ) and (2) A 1070nm, 200W (CW) fiber laser (SPI Lasers, Model: SP-200C-W-S6-A-B). The laser was directed by static mirrors into a scan head (ScanLab HurryScan 14mm) to allow for high-speed, two-dimensional scanning at beam velocities of up to 1.5m/s. The scan head was controlled by a Fore-Sight control card from LasX Industries and had an f-theta objective (Linos f-theta-Ronar, Model: 4401-302-000-20/21) with a focal length of 100mm. A z-axis manual stage was used to adjust the laser spot size (i.e., fluence incident on the sample) and to accommodate samples of varying thickness.

B. SAMPLES

Experimental surfaces on Ti6Al4V alloy were produced using micro end milling process. Micro end milling was done using a 2-flute, 1mm diameter WC tool at a spindle speed of 40,000rpm and 800mm/min feed rate corresponding to a chipload of 10μm. The average surface roughness, S_a, of such produced samples is 205.1±14nm.

C. PULSE DURATIONS[23]

The micro end milled samples were polished at three different pulse durations. The temporal characteristics were measured and are shown in Fig. 4. Note that the three temporal profiles are not uniform. Hence both the full width half maximum pulse duration (τ_H) and the 10% pulse duration (τ_{10}) are measured [23]. For the current paper, only τ_H will be used as reference. Fig. 4(a) shows the temporal profile for ~650ns pulses generated using the Nd:YAG laser in Q-switched mode at a pulse frequency of 4kHz. Figs. 4(b) and 4(c) show the pulse profiles generated by the fiber laser, with pulse durations of ~1.91μs and ~3.6μs, at frequencies of 40kHz and 25kHz respectively.

D. CROSS SECTIONS

For the measurement of the melt zone and heat affected zone (HAZ), samples were cut across the polished region, mounted, and mechanically ground and polished down to 3μm. The mechanically polished cross sections were ultrasonic cleaned in ethanol for 1min followed by chemical etching with a solution of ammonium bifloride (NH_4HF_2) for 1min. The etched cross sections were observed under an optical microscope, at 500x magnification.
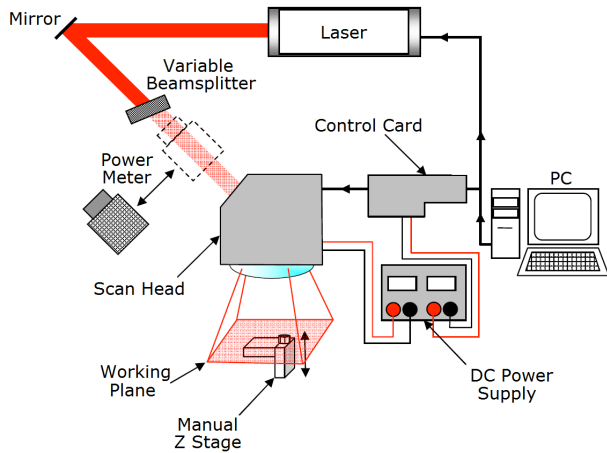

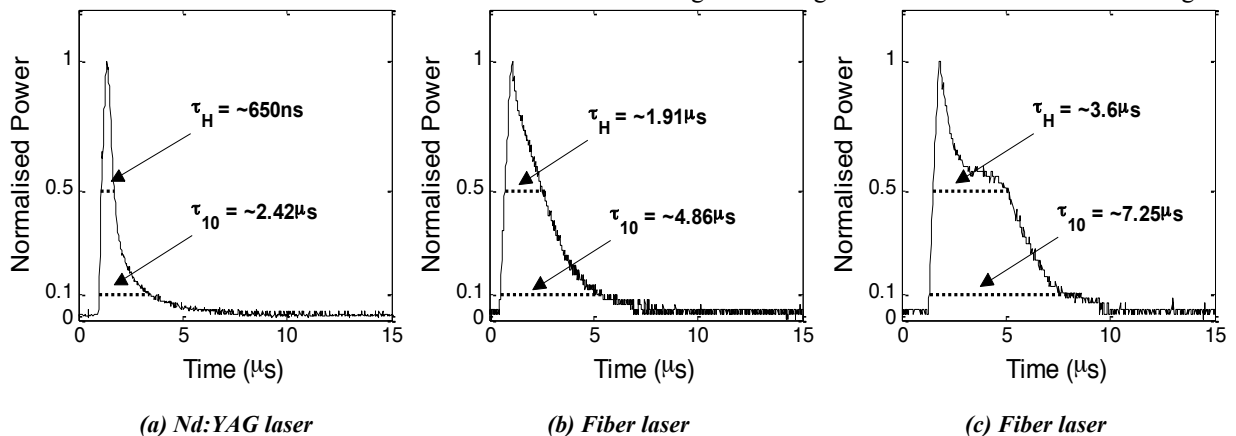**Fig. 3: Experimental setup**

E. POLISHING

The samples were polished near focus. The theoretical spot diameter at focus is ~60μm for the Nd:YAG laser and ~30μm for the fiber laser. The laser was scanned to follow a *zig-zag* pattern over an area of 1mm x 1mm. The laser scan speed is chosen so that spot overlap is approximately 80%. The line overlap of the raster is chosen to be approximately 50%. The polishing was done in an inert environment, to minimize oxidation and cracking of Ti6Al4V alloy.

EXPERIMENTAL RESULTS

PLμP was carried out on the sample surfaces at laser pulse durations of 650ns, 1.91μs and 3.6μs. Nd:YAG laser was used in Q-switched mode to generate the 650ns pulses at a frequency of 4kHz, while the fiber laser was used for 1.91μs and 3.6μs pulses at a frequency of 40kHz and 25kHz respectively. The polishing parameters are documented in Appendix A. The results of PLμP are tabulated in Table 3. Average roughness reductions up to 70% were achieved on both the samples. Fig. 5 shows 3D surface height data of the unpolished and the polished regions (350 μm x 265 μm) measured using the white light interferometer. A significant smoothening of the surface can be seen. The reader should note that the waviness was only filtered for the computation of S_a and that the 3D surface height plots show the actual data.

Fig. 6 shows the overlaid two-dimensional spatial frequency spectra of the unpolished and the polished surfaces. Figs. 6(a) and 6(b) are the projections of the spectra onto the two vertical planes, corresponding to the frequencies in the *x* and *y* directions respectively. Note that the low frequencies corresponding to the waviness were filtered using a high pass Gaussian filter with cut-off wavelength, λ_c = 0.08mm (f_c = 12.5 mm^{-1}) [21, 22]. Significant reduction in the amplitudes of the frequency components can be seen, especially at longer pulse durations. Spectra for all the three polishing conditions effectively remove the high spatial frequency (>100 mm^{-1}) components. The amplitudes of the low spatial frequency components (25–100 mm^{-1}) polished at 1.91μs and 3.6μs are smaller than the corresponding amplitudes polished at 650ns. This is an expected result as longer pulse durations result in longer melt durations, which means more time for the short frequency (long wavelength) spatial features to smooth out.

Figs. 7 through 9 show the cross section images of the

| (a) Nd:YAG laser | (b) Fiber laser | (c) Fiber laser |

Fig. 4: Temporal profiles of laser pulses at (a) 650ns (b) 1.91μs and (c) 3.6μs

polished samples. The melt depths, HAZ thicknesses and spot diameters were measured and are listed in Table 4. Note that there is no clear distinction between the melt zone and the HAZ for 650ns polishing (Fig. 7) and only the HAZ thickness could be measured. It is evident from the cross sections that longer pulse durations result in deeper heat affected zones.
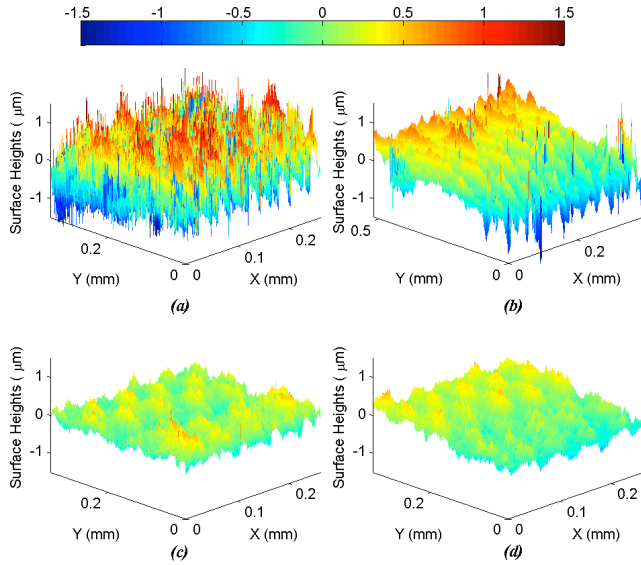

(a)   *(b)*

Fig. 7: Cross section images of (a) line, (b) area polished at 650 ns

(a)   *(b)*
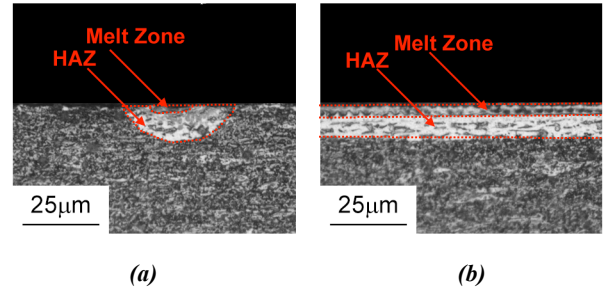
Fig. 8: Cross section images of (a) line (b) area polished at 1.91μs

(a)   *(b)*
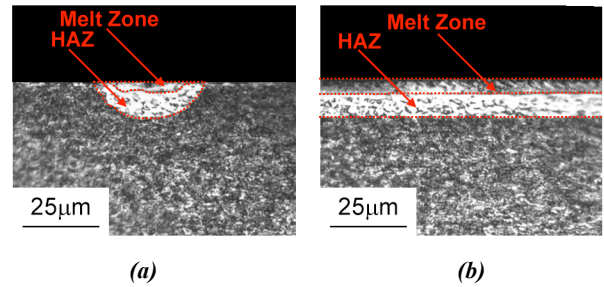
Fig. 9: Cross section images of (a) line, (b) area polished at 3.6μs

Table 3: Experimental (polished) roughness and reductions

Pulse duration (μs)	Sa-Unpolished (nm)	Sa-Polished (nm)	Reduction in Sa (%)
0.65	193.9	152.4	21.3
1.91	211.6	66.5	68.6
3.6	206.5	57.0	72.4

Table 4: Melt depths, HAZ thicknesses and spot diameters

Pulse duration (μs)	Melt Depth (μm)	HAZ thickness (μm)	Spot dia. (μm)
0.65	-	2.54	56.14
1.91	4.24	8.26	37.08
3.6	5.51	7.94	37.50

Fig. 5: 3D surface height data of the (a) Unpolished (b) Polished - 650ns (c) Polished – 1.91μs (d) Polished – 3.6μs
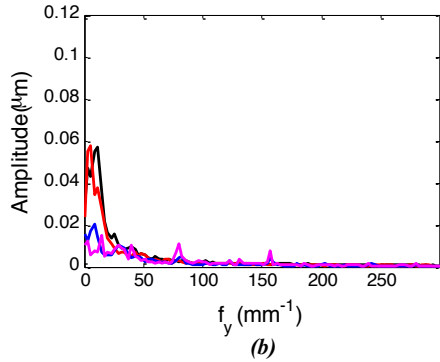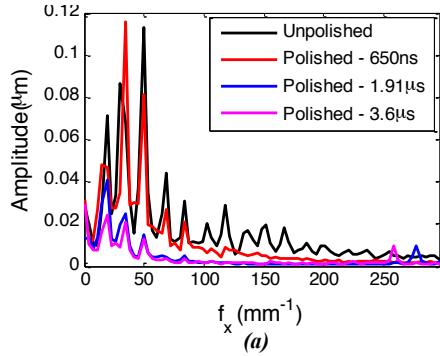

Fig. 6: Overlapped 2-D frequency spectra of unpolished, and polished (650ns, 1.91μs & 3.6μs). (a) Projected x-frequency spectra; (b) Projected y-frequency spectra
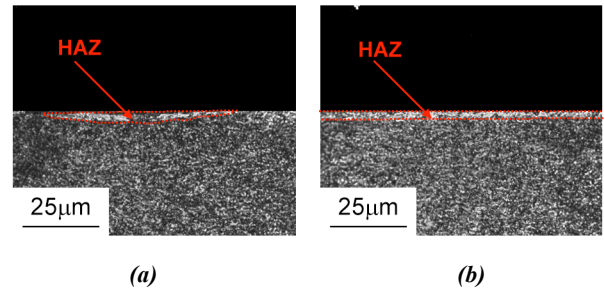
DISCUSSION

Figs. 10 through 12 show the overlaid spatial frequency spectra of the theoretically predicted polished surface and experimentally measured polished surface for the three pulse durations. The predictions of the average surface roughness, S_a, are presented in Table 2. It can be seen that the predicted spectra and S_a corresponding to 650ns match closely to the

experimental data, while there is a substantial difference in the theoretical and experimental spectra for the other two cases; i.e., 1.91μs and 3.6μs. It is also observed that additional features are introduced in the high frequency regions of the spectrum after polishing at 1.91μs and 3.6μs (Figs. 11 and 12). This feature corresponds to number of laser spots incident per mm in the scanning direction and zig-zag path laser line overlap in the direction perpendicular to the scanning. The spatial frequencies corresponding to these features were calculated for each case based on the processing parameters (Appendix A) and are listed in Table 5. Note that these features are absent on the surface polished at 650ns (Fig. 10). The introduction of these additional features is suggestive of the presence of convective flows.

Evidence of convective flows can be drawn from close observation of the cross section images (Figs. 8 and 9). The magnified images of the cross sections are shown in Fig. 13. In Figs. 13(a) and 13(b) (cross sections corresponding to polishing at 1.91μs and 3.6μs respectively), a surface ripple can be observed. The frequency of this ripple corresponds to the additional feature observed in the spatial frequency spectra (Figs. 11 and 12). The cross sections also suggest a flow pattern of the molten fluid, moving outwards from the center of the molten pool. The formation of such surface ripples is a confirmation of convective flows.
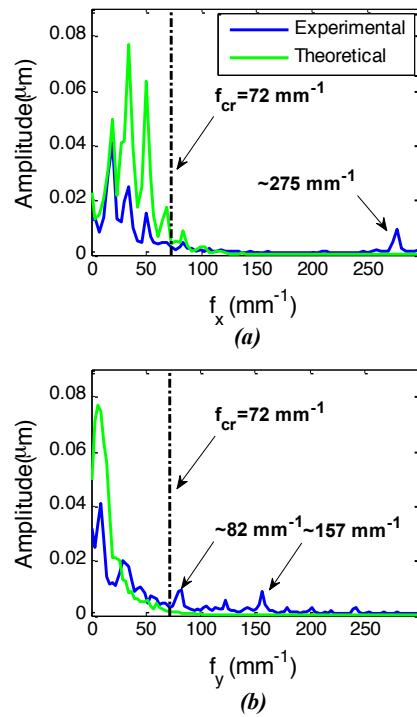

Fig. 11: Comparison of experimental (polished) and theoretical (predicted) 2-D frequency spectra at 1.91μs (a) Projected x-frequency spectra; (b) Projected y-frequency spectra
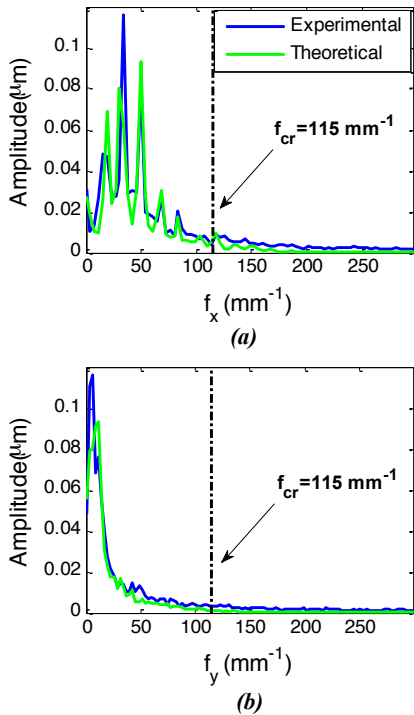

Fig. 10: Comparison of experimental (polished) and theoretical (predicted) 2-D frequency spectra at 650ns (a) Projected x-frequency spectra; (b) Projected y-frequency spectra
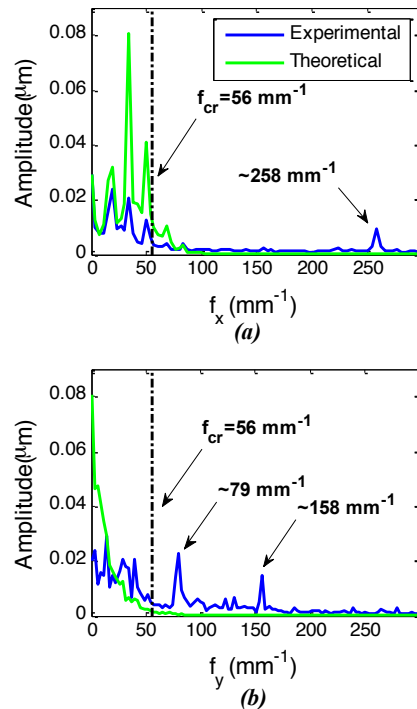

Fig. 12: Comparison of experimental (polished) and theoretical (predicted) 2-D frequency spectra at 3.6μs (a) Projected x-frequency spectra; (b) Projected y-frequency spectra
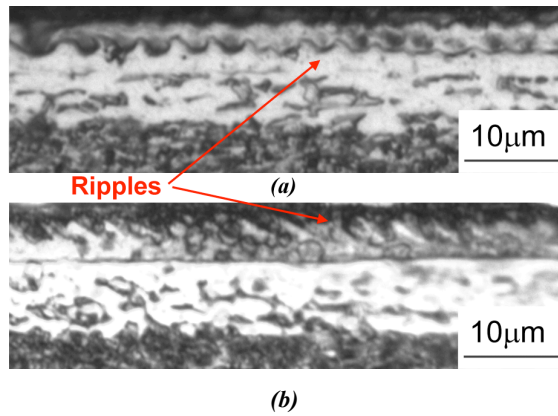
Fig. 13: Magnified cross section images showing surface ripples at (a) 1.91μs and (b) 3.6μs

Table 5: PLμP induced features

Pulse duration (μs)	Spatial frequency (mm⁻¹)	
	pulses/mm	Lateral overlap
0.65	133.33	83.3
1.91	266.7	77
3.6	250	77

Table 6: Comparison of experimental and theoretical roughness

Pulse duration (μs)	Experimental Sa (nm)	Theoretical Sa (nm)
0.65	152.4	138.0
1.91	66.5	127.5
3.6	57.0	94.4

As noted earlier, the theoretical model that was previously developed assumes that convective flows are negligible and that the dynamics of the melt pool are dominated by stationary capillary wave-like oscillations. This fundamental assumption is violated in the cases of 1.91μs and 3.6μs and hence, a large deviation is observed from the theoretical values. Further development of the model will be necessary to represent these flows, and this is beyond the scope of this paper.

However, convective flows are not necessarily an unfavorable phenomenon in pulsed laser micro polishing. It should be noted that greater than 70% reduction in the surface roughness was achieved at these longer pulse durations (Table 3). Even though convective flows introduced additional spatial features on the surface, they were also able to attenuate much lower frequency components, resulting in low surface roughness.

CONCLUSIONS

In the work presented, the effects of laser pulse duration on pulsed laser micro polishing (PLμP) process were observed. PLμP was carried out on micro end milled Ti6Al4V samples at three different pulse durations, viz. 650ns, 1.91μs and 3.6μs. Longer pulse durations resulted in smoother surfaces, with up to 70% reduction in average surface roughness, S_a.

While the experimental results for 650ns polishing matched very closely with those predicted theoretically, with an error less than 10%, the experimental roughness reduction was much higher than those predicted in the cases of 1.91μs polishing and 3.6μs polishing. Analysis of the two dimensional spatial frequency spectra revealed that at these pulse durations, the attenuation in the low frequency amplitude was much higher than those predicted theoretically. They also showed that additional features were introduced in high frequency regions corresponding to the number of pulses per mm. This suggests the possibility of convective flows. Convective flows were confirmed upon close observation of the cross sections of the polished samples, which showed a surface ripple at the same frequency as the number of pulses per mm. As the theoretical model presented assumes negligible convective flows, the model significantly deviated from the experimental results.

An important observation made from the current work is that the presence of convective flow may not be unfavorable for PLμP process, as up to 70% reductions in S_a were observed.

REFERENCES

[1] J. Martan, O. Cibulka, and N. Semmar, "Nanosecond pulse laser melting investigation by IR radiometry and reflection-based methods," *Applied Surface Science,* vol. 253, no. 3, 2006, pp. 1170-1177.

[2] W. E. Pendleton, G. P. Williams, R. T. Williams, J. C. Wu, G. B. Cvijanovich, J. L. Joyce, and M. McCleaf, "Scanning Tunneling Microscopy of Nickel Surface Features Before and After Rapid Melting by Excimer Laser," *AMP Journal of Technology,* vol. 3, 1993, pp. 75-84.

[3] A. Lamikiz, J. A. Sanchez, L. N. L. de Lacalle, D. del Pozo, and J. M. Etayo, "Surface roughness improvement using laser-polishing techniques," *Advances in Materials Processing Technologies,* vol. 526, 2006, pp. 217-222.

[4] J. A. Ramos-Grez, and D. L. Bourell, "Reducing surface roughness of metallic freeform-fabricated parts using non-tactile finishing methods," *International Journal of Materials & Product Technology,* vol. 21, no. 4, 2004, pp. 297-316.

[5] E. Willenborg, K. Wissenbach, and R. Poprawe, "Polishing by laser radiation," in *Proceedings of the Conference*, 2003.

[6] P. F. Marella, D. B. Tuckerman, and R. F. Pease, "Modelling of Laser Planarization of Thin Metal-Films," *Applied Physics Letters,* vol. 54, no. 12, 1989, pp. 1109-1111.

[7] D. B. Tuckerman, and A. H. Weisberg, "Planarization of Gold and Alumunum Thin-Films using a Pulsed Laser," *Ieee Electron Device Letters,* vol. 7, no. 1, 1986, pp. 1-4.

[8] A. Temmler, K. Graichen, and J. Donath, "Laser Polishing in Medical Engineering; Laser Polishing of Components for Left Ventricular Assist Devices," *Laser Technik Journal,* vol. 7, no. 2, 2010, pp. 53-57.

[9] M. Bereznai, I. Pelsoczi, Z. Toth, K. Turzo, M. Radnai, Z. Bor, and A. Fazekas, "Surface modifications induced by ns and sub-ps excimer laser pulses on titanium implant material," *Biomaterials,* vol. 24, no. 23, 2003, pp. 4197-4203.

[10] Y. G. Kim, J. K. Ryu, D. J. Kim, H. J. Kim, S. Lee, B. H. Cha, H. Cha, and C. J. Kim, "Microroughness reduction of tungsten films by laser polishing technology with a line beam," *Japanese Journal of Applied Physics Part 1-Regular Papers Short Notes & Review Papers,* vol. 43, no. 4A, 2004, pp. 1315-1322.

[11] T. L. Perry, D. Werschmoeller, X. Li, F. E. Pfefferkorn, and N. A. Duffie, "Pulsed laser polishing of micro-milled Ti6Al4V samples," *Journal of Manufacturing Processes,* vol. 11, no. 2, 2009, pp. 74-81.

[12] T. L. Perry, D. Werschmoeller, X. C. Li, F. E. Pfefferkorn, and N. A. Duffie, "The Effect of Laser Pulse Duration and Feed Rate on Pulsed Laser Polishing of Microfabricated Nickel Samples," *Journal of Manufacturing Science and Engineering-Transactions of the Asme,* vol. 131, no. 3, 2009.

[13] T. L. Perry, D. Werschmoeller, N. A. Duffie, X. C. Li, and F. E. Pfefferkorn, "Examination of Selective Pulsed Laser Micropolishing on Microfabricated Nickel Samples Using Spatial Frequency Analysis," *Journal of Manufacturing Science and Engineering-Transactions of the Asme,* vol. 131, no. 2, 2009.

[14] M. Vadali, C. Ma, N. A. Duffie, X. Li, and F. E. Pfefferkorn, "Pulsed Laser Micro Polishing: Surface Prediction Model," in *Proceedings of the International Conference on MicroManufacturing (ICOMM) Conference,* 2011, pp. 331-338.

[15] L. D. Landau, and E. M. Lifshits, Fluid mechanics, Editor: 1959, pp. Pages.

[16] C. Nüsser, I. Wehrmann, and E. Willenborg, "Influence of Intensity Distribution and Pulse Duration on Laser Micro Polishing," *Physics Procedia,* vol. 12, Part A, no. 0, 2011, pp. 462-471.

[17] A. Bagno, M. Genovese, A. Luchini, M. Dettin, M. T. Conconi, A. M. Menti, P. P. Parnigotto, and C. Di Bello, "Contact profilometry and correspondence analysis to correlate surface properties and cell adhesion in vitro of uncoated and coated Ti and Ti6Al4V disks," *Biomaterials,* vol. 25, no. 12, 2004, pp. 2437-2445.

[18] V. Borsari, G. Giavaresi, M. Fini, P. Torricelli, A. Salito, R. Chiesa, L. Chiusoli, A. Volpert, L. Rimondini, and R. Giardino, "Physical characterization of different-roughness titanium surfaces, with and without hydroxyapatite coating, and their effect on human osteoblast-like cells," *Journal of Biomedical Materials Research Part B-Applied Biomaterials,* vol. 75B, no. 2, 2005, pp. 359-368.

[19] D. Khang, J. Lu, C. Yao, K. M. Haberstroh, and T. J. Webster, "The role of nanometer and sub-micron surface features on vascular and bone cell adhesion on titanium," *Biomaterials,* vol. 29, no. 8, 2008, pp. 970-983.

[20] L. Ponsonnet, K. Reybier, N. Jaffrezic, V. Comte, C. Lagneau, M. Lissac, and C. Martelet, "Relationship between surface properties (roughness, wettability) of titanium and titanium alloys and cell behaviour," *Materials Science & Engineering C-Biomimetic and Supramolecular Systems,* vol. 23, no. 4, 2003, pp. 551-560.

[21] "Surface Texture: Surface Roughness, Waviness, and Lay; ASME B46.1-2009 (Revision of ASME B46.1-2002)," Amer Society of Mechanical, 2009.

[22] ISO, "ISO 16610-21, Geometrical product specifications (GPS) -- Filtration -- Part 21: Linear profile filters: Gaussian filters," 2011.

[23] ISO, "ISO 11554:2006, Optics and photonics -- Lasers and laser-related equipment -- Test methods for laser beam power, energy and temporal characteristics," 2006.

Appendix A: PLµP Process Parameters

650ns	Type of laser	250 W CW Nd:YAG
	Pulse frequency (kHz)	4
	Spot size (µm)	~55
	Scan speed(mm/s)	30
	Average power (W)	0.46±0.03
	Energy per pulse (mJ)	0.115±0.008
	Melt duration (ns)	1164
	Critical frequency (mm^{-1})	115
1.9µs	Type of laser	200 W CW/Modulated Fiber Laser
	Pulse frequency (kHz)	40
	Spot size (µm)	~37
	Scan speed(mm/s)	150
	Average power (W)	3.88±0.05
	Energy per pulse (mJ)	0.097±0.001
	Melt duration (ns)	2980
	Critical frequency (mm^{-1})	72
3.6µs	Type of laser	200 W CW/Modulated Fiber Laser
	Pulse frequency (kHz)	25
	Spot size (µm)	~37
	Scan speed(mm/s)	100
	Average power (W)	3.16±0.02
	Energy per pulse (mJ)	0.126±0.001
	Melt duration (ns)	4982
	Critical frequency (mm^{-1})	56